

# Investigation of Structural and Modal Analysis of a Wind Turbine Planetary Gear Using Finite Element Method

Abdellah Mohsine\*<sup>‡</sup>, Boudi El Mostapha\*, Abdellatif El Marjani\*

\*EMISys Research Team, Engineering 3S Research Center, Mohammadia School of Engineers, University Mohammed V in Rabat, Morocco.

Abdellah Mohsine: +212 606 103 638

<sup>‡</sup>For correspondence: Email: mohsine.abdellah@gmail.com

*Received: 31.12.2017 Accepted:11.02.2018*

**Abstract**-Damages in gears may result from excessive operating load (overload), inadequate operating conditions, operation near the resonant frequency of a gear structure, or simple fatigue during power transmission. In mechanical design, the engineers must always ensure that the mechanical resonance frequencies of the components are not allowed to match the drive oscillation frequencies of oscillating parts. Various experimental and theoretical techniques have been developed to analyze such vibrational problems. In this paper, the planetary gear was modeled in Pro/ENGINEER Wildfire 4.0 while the Mesh and the structural, modal and response harmonic analysis for different boundary conditions were performed in ANSYS Workbench 15.0. A modal analysis was then performed for these different cases to calculate a few initial natural frequencies and to analyze its movements using the harmonic response. Furthermore, it is observed that the value of the maximum occurred stress obtained by the harmonic response analysis for the three different cases is less than the maximum materials stress.

**Keywords:** planetary gear; structural analysis; frequency; modal; harmonic.

## 1. Introduction

It has become clear that fossil fuel reserves are not infinite and that their forced combustion is creating insurmountable and increasingly serious environmental problems[1]. For this reason, and for economic reasons, designers and decision-makers in the electrical industry must provide solutions to improve the current situation and reduce destructive environmental effects[2]. It will be necessary to learn how to do without fossil fuels, which still represent a major demand of energy in the world, and to develop the renewable energies where wind energy has a major role to play in this process where many researchers have been able to put their skills and know-how to find sustainable solutions[3], [4]. Large wind turbines are dynamically loaded along the entire chain, which transforms the slow rotation of the main shaft into rapid rotation to serve the electrical power in the electricity network. For this reason and despite the technology evolution, gearbox dysfunction is one of the most common causes of energy loss[5].

Planetary gears are fundamental parts of many accuracy power transmission elements such as an automobile, tractors, wind turbines, helicopters, and aircraft engines, where high torque to weight ratios, large speed reductions

and multiplications in compact volumes, co-axial shaft arrangements, high reliability and superior efficiency are

required[6]. Gear vibrations and stresses are main worries in most planetary gear transmission mechanisms, where the obvious problem may be noise or dynamic forces[7].

The used planetary gear is an epicycle gear structure that contains four main components: a sun gear, three planet gears that rotate round their axis and around the sun gear, a support or carrier on which the planets are held and rotating and an internal gear that is meshed with the planet gears. In this case the force is transmitted from the planet carrier also via the planet gears to the sun gear.

The conception and simulation of such mechanism are very important to guess the actual action behavior. When designing gears, the response of the gear train dynamic is considered as critical[8]. Modal response is a dynamic response from the gear in the form of periodic excitations such as in noise analysis, and structural response to vibration. The modal analysis can anticipate the resonance of the structure, which is stimulated by the dynamic input. In this condition, the mechanical stress level can become very high and create structural inadequacies. Sinisca[9] analyzed the modal analysis of the double-stage helical gear

using finite element simulation via free and forced response.

Dynamic tooth and bearing loads influence the life times of planetary gear parts. Vibration can cause structural failure in mechanical engines. Planetary gears fail in wind turbine due to dynamic loads and vibrations coming from gear excitations[10][11].

Lin and Parker[12]strictly analyzed the natural frequency spectrum and vibration modes of planetary gear systems involving a lumped parameter model.

The research literature about the planetary gear boxes focuses on the modeling of high idealized lumped parameter where the gears are considered as rigid bodies connected by springs representing meshing teeth for free vibration analyses, see[7], [12]–[17].

A. Kahraman[18], [19] worked on two and three dimensional models to study the dynamic response of time invariant and time varying representations. Flamand and Velex[18], [19] used lumped modeling[20], and a Ritz approach to examine the dynamic response induced by mesh parametric excitations. The gear bodies in all these studies are represented by lumped parameter models. Valco [16] [20]used a non-linear FE model of a planetary gear system to compute stress, displacement and deformation in the gear bodies under static loading. Dynamic response is not taken in consideration. Gradu et al. [17] used a FE model to obtain the dynamic response of various planetary gear systems with different planet spacings.

This paper presents the steps completed in order to determine the natural frequencies and stress distributions on the gears trough FEM simulations. The parts submitted to simulation were chosen considering the three boundary conditions. The sun, the carrier, the three planets and the internal gear were submitted to simulations. The FEM were performed using ANSYS 15.0 Simulation software and have involved the following steps:

- ✓ 3D modeling of the components geometry using Design Software Pro/ENGINEER Wildfire 4.0 of the PTC (Parametric Technology Corporation);
- ✓ Exporting the assembly from Pro/ENGINEER Wildfire 4.0 in IGES format and importing it in ANSYS simulation program (ANSYS 15.0);
- ✓ Defining a FEM static study;
- ✓ Assigning material properties;
- ✓ Defining the loads for the structural simulation;
- ✓ Generating the mesh;
- ✓ Running the study;
- ✓ Analysis of the results.

For the involute profile of the teeth we are used curves driven by the parametrical equation of the involute curve: Fig. 1 illustrates the planetary gear used in this study. In this particular planetary gear, the input is the planet carrier, the ring gear is stationary, and the output is the sun gear.

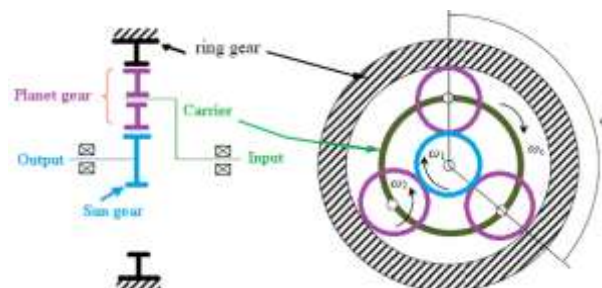


Fig.1. The planetary gear used in this study.

## 2. Geometry

### 2.1. Dimensioning variables

The dimensioning of a gear requires at least 3 parameters: the number of teeth  $Z$  (or the pitch diameter  $d$ ), the modulus  $m$  and the pressure angle  $\alpha$ . From this data, it is possible to deduce the pitch, the exact dimensions of the teeth as well as the axis-to-axis distance of the two gears. The basic data are given in the table below[21].

Table 1. Calculation of Gear Parameters

Specification	ISO-Symbol	Formulas	Satellite (P)	Sun (S)	Ring (C)
Module	m	Standard values	1.5	1.5	1.5
Pitch primitive	P	$P = \pi m$	4.71	4.71	4.71
Number of teeth	Z		40	20	100
Pitch diameter	D	$D = mZ$	60	30	150
Foot diameter	$D_f$	$D_f = D - 2.5m$ ; $D_f = D + 2.5m$ (C)	56.25	26.25	153.75
Head diameter	$D_a$	$D_a = D + 2m$ ; $D_a = D - 2m$ (C)	63	33	147
Base diameter	$D_b$	$D \cos \alpha$	56.38	28.19	140.95
Tooth width	b	$B = Km$ $K=10$	15	15	15
Tooth height	h	$H = h_a + h_f = 2.25m$	3.38	3.38	3.38
Tooth thickness	E	$E = \pi m / 2$	2.34	2.34	2.34

Pressure angle	$\alpha$		20°	20°	20°
----------------	----------	--	-----	-----	-----

2.2. Multiplication factor of the planetary gear

Since the ring is fixed, the satellite carrier angular velocity is:

$$\omega_{PS} = 100 \frac{rd}{s}, Z_S = 20, Z_P = 40, Z_C = 100$$

The angular velocity  $\omega_S$  of the main wheel (S) can also be found using the following:

$$\frac{\omega_{sortie}}{\omega_{entrée}} = \frac{\omega_S}{\omega_{PS}} = \frac{Z_S + Z_C}{Z_S}$$

$$\omega_S = \omega_{PS} \frac{Z_S + Z_C}{Z_S}$$

$$\omega_S = 100 \frac{20 + 100}{20} \left(\frac{rd}{s}\right)$$

$$\omega_S = 600 \frac{rd}{s}$$

Also the multiplication factor of the used planetary gear is 6.

2.3. Design of a planetary gear train

The software used for the design of the planetary gear is Pro/ENGINEER Wildfire 4.0 of the PTC (Parametric Technology Corporation). The assembly created is saved as IGES format and transferred to the ANSYS Workbench simulation program.

The planetary gear must have the following construction: A main wheel the sun (S), three satellites (P), satellite carrier (PS) and a ring type wheel the crown (C). In most operating modes of a planetary gear train, at least one of the parts (the main wheel, the satellite, and the crown or satellite carrier) is fixed.

3. Part Design

3.1. The involute circle

After establishing the characteristic diameters ( $D, D_b, D_a$  and  $D_p$ ), the next step is to create the involute circle whose parametric equations are written as following in Pro/ENGINEER Wildfire 4.0:

$$\begin{aligned} \text{Base\_circle\_radius} &= 28.2/2 \\ \text{Angle} &= t * 90 \\ \text{Cir\_len} &= (PI * \text{Base\_circle\_radius} * t)/2 \\ X_{INS} &= \text{Base\_circle\_radius} * \cos(\text{Angle}) \\ Y_{INS} &= \text{Base\_circle\_radius} * \sin(\text{Angle}) \\ X &= X_{INS} + (\text{Cir\_len} * \sin(\text{Angle})) \\ Y &= Y_{INS} - (\text{Cir\_len} * \cos(\text{Angle})) \\ Z &= 0 \end{aligned}$$

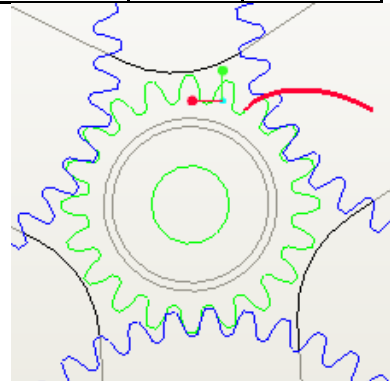
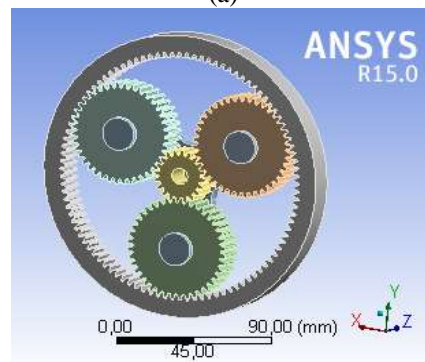


Fig.2. Involute curve from circle equations.

Once the involute circle is defined, it remains to transfer all the respective diameters and to apply the successive transformation operations of the basic sketch (Fig. 2). At the end of this design process, the final model (Fig. 3) is ready to be transferred to ANSYS 15.0. Note that the model has been simplified because of the numerous symmetries and repetitions present on it. All gears (sun, satellite and ring) are modeled following the same gear design parameters shown in Table 1. The material properties are the same for all gears Hardening, tempering and other gear heat treatment processes are not considered in this study. Therefore, only the gear material will be considered in the FEM analysis.



(a)



(b)

Fig. 3. (a): Model geometry in Pro/ENGINEER Wildfire. (b): Planetary gear geometry imported in Ansys.

**Table 2:** Geometry Data

Planetary gear properties	
Volume	2.7904e+005 mm <sup>3</sup>
Mass	2.1904 kg
Length following X	175 mm
Length following Y	175 mm
Length following Z	48 mm

#### 4. Static Analysis

There are more research and many books about gear analysis that have been published. The gear static and dynamic analysis, transmission errors, gear noise and the optimal shape of gear trains are still the main concerns in the gears design. Errichello[22] has studied a large part of the literature on the development of various simulation models for static and dynamic analysis of different gear types[23][24].

Static stress analysis using FEM was performed on the standard planetary gear with 3 satellites considering the three different boundary conditions, focusing mainly on the gear tooth stress and contact stress caused by the contacting gear teeth. The three boundary conditions are analyzed separately.

##### 4.1. Simulating the behavior of a planetary gear

The simulation is performed by ANSYS 15.0. The axis entered (satellite carrier) is driven with a torque of 200 Nm. The dimensions of the toothed wheels and the axis of the planet carrier are shown in Table above. In this case the system is considered as static.

The mechanical behavior of the planetary gears is analyzed by the numerical method. The stresses and strains of the planetary gears are obtained by numerical analysis. The results provide a theoretical basis for the analysis of the structure and system optimization type.

The involute spur gears are the most common form of gears that are used to transfer motion between parallel shafts.

##### 4.2. Mesh

A three-dimensional (3D) model of the planetary gear was modeled. A single pair tooth contact between gears was carefully aligned using PTC Software Pro/ENGINEER Wildfire 4.0. Tetrahedron element was chosen to build the FE mesh model of the planetary gear.

The pair tooth contact was aligned touching each other tangentially. The contact surface between gears was set to be rigid contact selecting the option “No Separation” contact, which is also considered as linear contact.

With the finite element method, many contact problems, from the simplest to the most complicated, can be solved with great precision. The FEM can be considered as the preferred method for dealing with contact problems because of its success in handling with mechanical problems in the field of solid mechanics, fluids, heat transfer and field problems[25].

This step consists of the finite element decomposition of the model. The smaller the mesh size, the finer the accuracy, the greater the resolution time. It is preferable to select the automatic method in order to have standard results. The Fig. 4 illustrates the planetary gear mesh automatically performed by the software ANSYS 15.0.

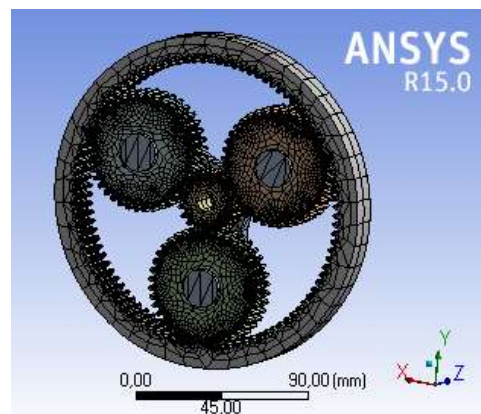


**Fig. 4.** Mesh model of planetary gear FE simulation.

##### 4.3. Boundary conditions

ANSYS Workbench was used to apply the constraints and boundary conditions. There are three different conditions being considered and analyzed for the static, modal analysis and harmonic response of the planetary gear as shown in Fig. 5. In the first section of this study, stress, displacement and deformation of the planetary gear will be calculated. In the second section the modal analysis and in the latest section the harmonic response will be analyzed.

- ✓ **Condition 1:** The sun is fixed for power transmission output (case 1). The input movement comes from the ring and goes into the satellite and then to the carrier. The sun is considered as idler.
- ✓ **Condition 2:** The carrier is fixed for power transmission output (case 2). The input movement comes from the sun and goes over the satellite into the ring: Speed reducer
- ✓ **Condition 3:** The ring is fixed for power transmission output (case 3). The input movement comes from the carrier and goes over the satellite into the sun: Speed multiplier



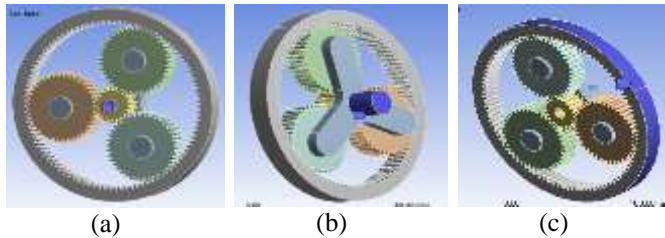


**Fig.5.** Three Boundary conditions set on the planetary gear.(a) Case 1: sun fixed, (b) Case 2: Carrier fixed, (c) Case 3: Ring fixed.

4.4. Applied Load for each case.

According to the three boundary conditions that are mentioned in the preceding paragraph, we have also three cases to study concerning the applied loads.

- ✓ Case 1: The sun is fixed as shown in Fig. 5 (a). To create a torque, a moment of 200 Nm was applied on the face of the ring. In addition, it is also necessary to unblock the carrier planet by releasing the tangential displacement cylindrical.
- ✓ Case 2: The carrier is fixed as shown in Fig. 5 (b). A Moment was applied on the sun and was the same as in case 1.
- ✓ Case 3: The ring is fixed as shown in Fig. 5(c). The same Moment value was applied on the shaft of the carrier

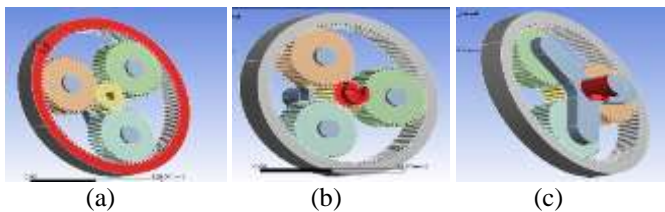


**Fig. 6.** Applied loads conditions. (a): sun fixed. (b): Carrier fixed. (c): Ring fixed.

4.5. Material properties:

Standard Steel	
Density Kg/m <sup>3</sup>	7850
Young's modulus MPa	2.e+005
Poisson's ratio	0.3

5. Results

The final step in this analysis is getting the results. The software gives a schematic solution according to the type of resolution. In the case of this analysis, we will limit ourselves to having solutions concerning the displacement, deformation and constraint of the planetary gear. Fig. 7 shows the graphical representation of deformation, Stress and displacement for the known three boundary conditions. For the case when the sun is fixed the maximal deformation and the maximal stress occurs at one side of the root fillet of the sun gear. When the carrier is fixed the maximal deformation and maximal stress occur at the gear teeth.

When the ring is fixed the maximal deformation and maximal stress occur at the sharp corner of the carrier shaft.

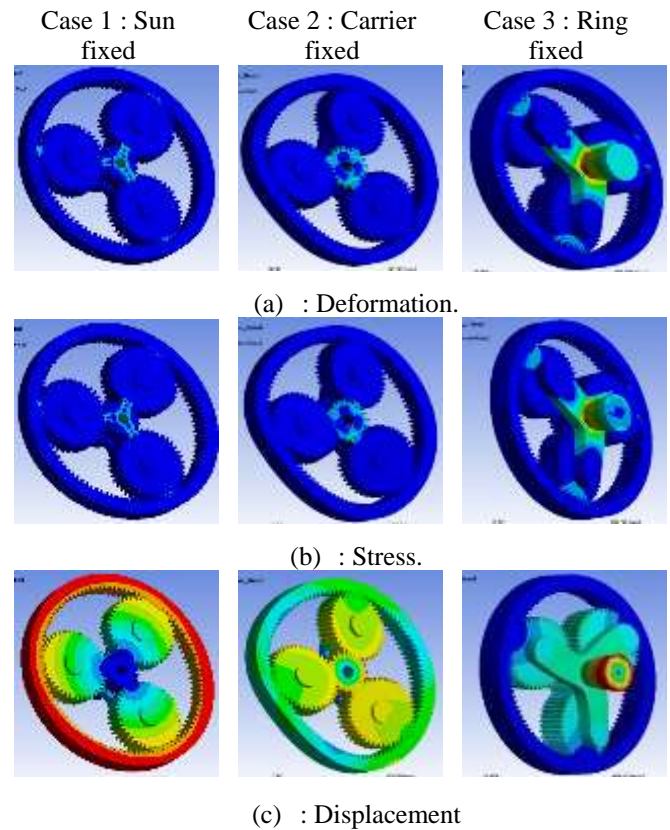


**Fig.7.** Deformation, (a) Von Mises Stress, (b) and Displacement, (c) of the planetary gear in three boundary conditions.

**Table 3:** Minimal and Maximal Values of The Deformation, Stress and Displacement

Case		Deformation (mm/mm)	Stress (MPa)	Displacement (mm)
1	Min	1.0235e-007	1.9071e-002	0
	Max	2.9948e-003	596.44	0.24693
2	Min	0	0	0
	Max	2.9056e-003	580.59	5.4269e-002
3	Min	1.4396e-010	1.1722e-005	0
	Max	6.7225e-004	122.31	2.0009e-002

6. Modal Analysis

Modal analysis, which studies the mode shape of structure under excitation of its own frequency, is important in the design phase. The modal analysis of the planetary gear with different combinations of boundary conditions has been analyzed under conditions of free stress, also the mode shapes of the planetary gear have been calculated independently of the excitation using FEM, which means that the structure depends solely on mass and stiffness.

After carrying out the static study of the system, we will proceed to the vibratory study. In a first step, we will perform the modal analysis of each case to obtain their respective natural frequencies of the planetary gear, and

then we will pass to the harmonic analysis to quantify the amplitude of the displacement of each case to the vibration.

6.1. Modal response

The matrix dynamic equation of motion for the lumped-parameter system using FEM is:

$$|M|\{\ddot{u}\} + |C|\{\dot{u}\} + |K|\{u\} = \{F\} \quad (1)$$

With:

- |M| is the mass matrix.
- |C| is the damping matrix
- |K| is the stiffness matrix.
- {ü} is the acceleration vector as a function of time.
- {u̇} is the velocity vector as a function of time.
- {u} is the displacement vector as a function of time.
- {F} is the load vector.

In general the damping value for most structures is less than 10%, so that the damping expression in the equation (1) can be neglected.

$$|M|\{\ddot{u}\} + |K|\{u\} = \{F\} \quad (2)$$

The mass M and stiffness K are the main properties that affect the overall modal response of a system. In general, when there is no excitation, the differential equation of motion (2) for a vibrating system always looks like this [38]:

$$|M|\{\ddot{u}\} + |K|\{u\} = \{0\} \quad (3)$$

The solution of equation (3) is of the form:

$$\{u\}(t) = \{U\}e^{i\omega t} \quad (4)$$

$$\{\ddot{u}\}(t) = -\omega^2\{U\}e^{i\omega t} \quad (5)$$

With

- {U} is the Eigen vector.
- $e^{i\omega t}$  is the temporal response that is simply a sinusoidal.
- $\omega$  is the radial frequency of the Sinusoidal.

Using equation (4) and (5) in (3), we obtain:

$$-\omega^2[M]\{U\}e^{i\omega t} + [K]\{U\}e^{i\omega t} = \{0\} \quad (6)$$

Dividing by  $e^{i\omega t}$  results in the eigenvalue equation:

$$([K] - \omega^2[M])\{U\} = \{0\} \quad (7)$$

A natural frequency is a frequency at which a free structure vibrates when it is in action. It has been found that the stress caused by vibrations is critical when resonances occur in the gear, since this can lead to catastrophic failure.

The use of the FEM for performing the modal analysis is considered to be advantageous because the analyzed gear structure can have any aspect and the results are acceptable and admissible[26].

7. Modal Analysis Results

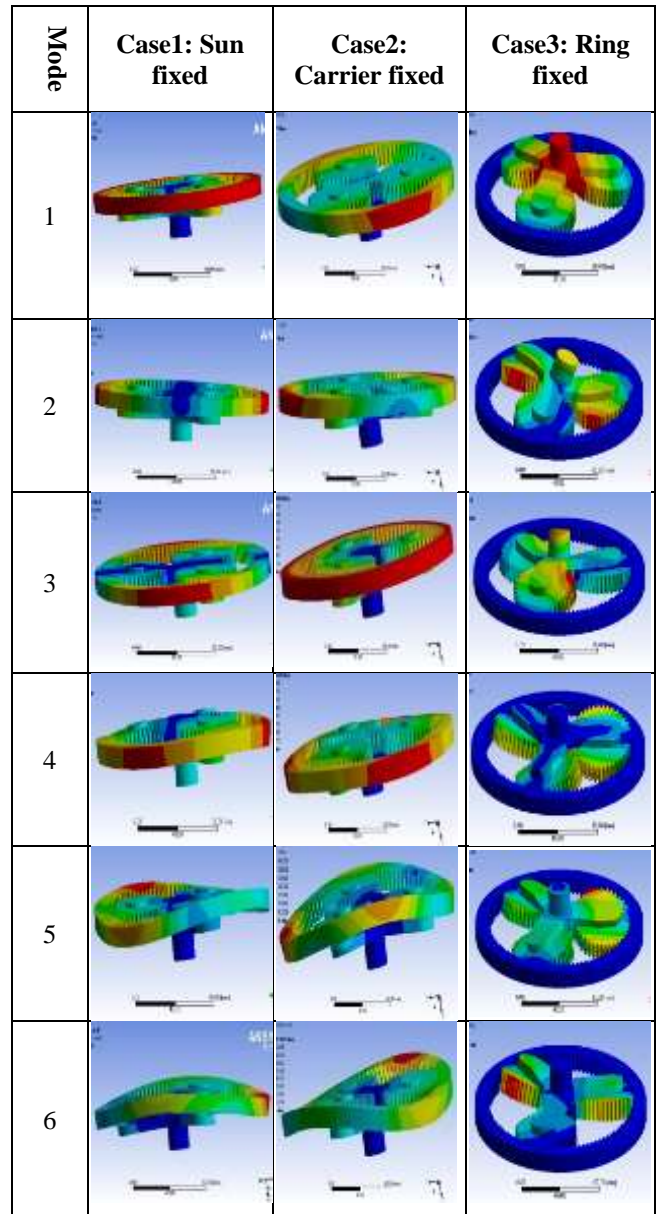
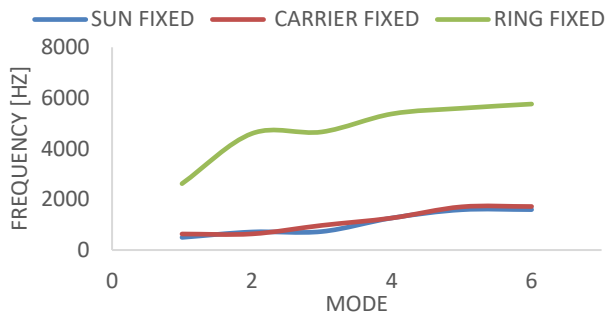


Fig. 8. Six mode shapes of the planetary gear for the three boundary conditions.

For a better overview, the following table shows all conditions with all variants and their associated frequencies (Hz) and displacement (mm). It was observed that the frequencies at the Ring fixation go on maximum in comparison to the other both cases.

Table 4. Calculated frequencies of the planetary gear for the Three body conditions using ANSYS

Mode	Frequency Hz		
	Sun fixed	Carrier fixed	Ring fixed
1	497.62	633.29	2618.5
2	712.1	636.85	4596.1
3	730.44	972.71	4660.5
4	1263.8	1263.4	5371.6
5	1590.2	1705.2	5594.3
6	1594	1717.3	5761.1



**Fig. 9.** Natural frequencies for the three boundary conditions.

The Fig. 9 shows the different calculated frequencies of the planetary gear for the three boundary conditions. It can be seen that the frequencies are almost the same for the both cases where the sun and the carrier are fixed while the higher frequencies appear in the case where the ring is fixed.

**Table 5.** Calculated displacements of the planetary gear for the Three body conditions using ANSYS

Mode	Displacement		
	Case 1 : Sun fixed	Case 2 : Carrier fixed	Case 3 : Ring fixed
1	32.8 mm	47.307 mm	39.831 mm
2	48.054 mm	45.37 mm	62.273 mm
3	47.042 mm	33.306 mm	54.725 mm
4	39.731 mm	37.558 mm	64.203 mm
5	60.4 mm	57.004 mm	76.31 mm
6	64.636 mm	59.702 mm	90.409 mm

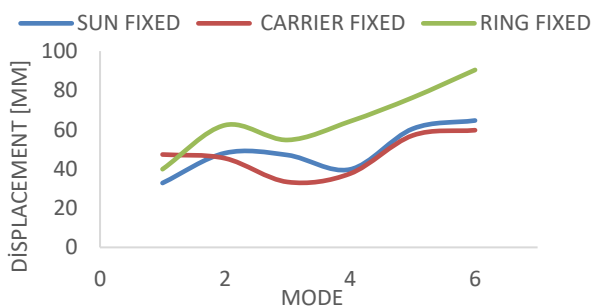


**Fig.10.** Displacement of the planetary gear for the three boundary conditions

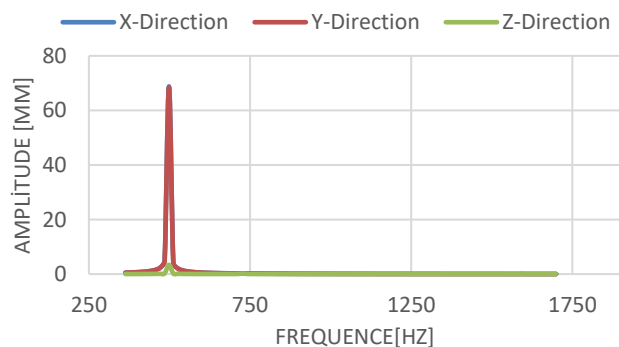
The Fig. 10 shows the displacements of the planetary gear for the three boundary conditions. We can see that the three cases have a similar behavior in terms of displacements. The maximum displacement occurs in z-axis when the ring is fixed.

### 8. Harmonic Response

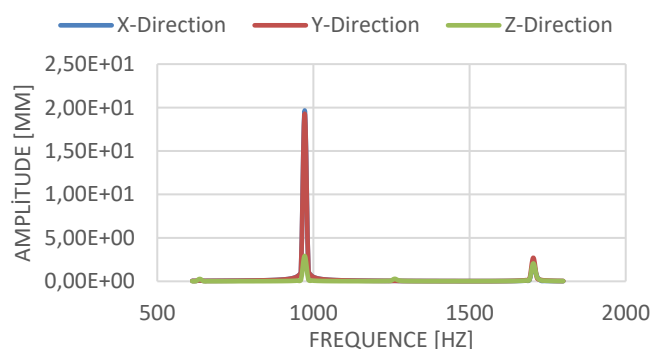
The harmonic response analysis, contrary to the modal analysis, allows us to define the amplitude of displacement and stress of the system due to the vibration for a given frequency already determined[27]. In this sense we have 3

cases studied according to the limiting conditions that we have fixed before.

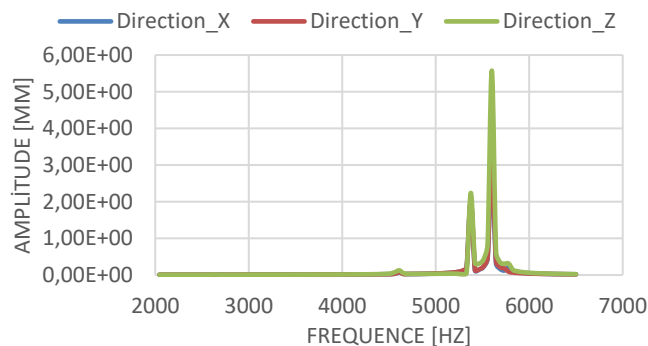
The amplitude spectrums of the different cases are shown in the following figures.



(a)



(b)



(c)

**Fig. 11.** Displacement of the planetary gear in x-, y- and z-direction for the three boundary conditions, (a): Displacement Sun Fixed, (b): Displacement Carrier Fixed, (c): Displacement Ring fixed.

Fig. 11 shows the displacements of the planetary gear in 3 directions x, y and z for the 3 boundary conditions. It should be noted that during the Sun fixation (a) and carrier fixation (b) the maximum displacements occur in y-axis and is respectively 68.332mm for the resonant frequencies between 450 and 512 Hz and 19.665mm for the resonant frequencies that are between 924 and 996 Hz, while the maximum displacement at the ring fixation (c) occurs in z-axis and is 5.58 mm for the resonant frequencies between 5150 and 5800 Hz. This is due to the fact that the sun and the carrier are within the ring and since this is fixed, the



movement of the inner parts (sun and carrier) can then only take place in the z-axis.

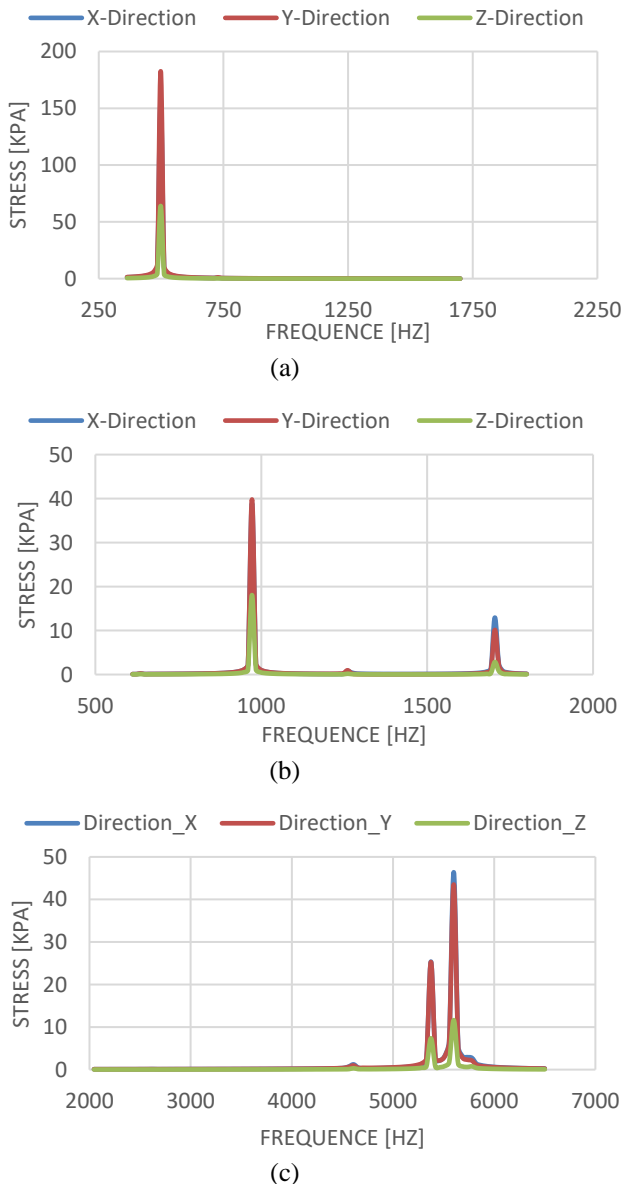


**Fig. 12.** Stress of the planetary gear in x-, y- and z-direction for the three boundary conditions, (a): Stress Sun Fixed, (b): Stress Carrier Fixed, (c): Stress Ring fixed.

Fig. 12 shows also the graphical representation of the stress of the planetary gear in 3 directions x, y and z for the 3 boundary conditions. For the case where the sun is fixed (a) the maximum stress occurs in y-axis and is 182.620 MPa for the resonant frequencies between 450 und 512 Hz, while at the carrier fixation (b) the maximum stress is 39.797 MPa in y-axis for the resonant frequencies between 924 and 996 Hz. When the Ring is fixed, the maximum stress in z-axis is 46.397 MPa for the resonant frequencies between 5150 and 5800 Hz.

From this result, the value of the maximum occurred stress obtained for the three different cases is less than the maximum materials stress.

**9. Conclusion:**

From the response harmonic analysis study, based on the results of the modal analysis of our planetary gear, we obtained the displacement and stress of different nodes of the system over the entire frequency range between 300 Hz and 1700 Hz for the case where the sun is fixed, and the range 600 Hz and 1800 Hz for the case where the carrier is fixed, and in the third case where the Ring is fixed the frequencies are between 2000 Hz and 6500 Hz. The peaks appeared in the Fig.11 and 12 show the amplitude of the displacement and stress that is maximum at the sides of the resonant frequencies which is logical since the destabilization generally exists on the side of the resonance frequencies.

**References**

- [1] S. R. S et V. Ramesh, « A Novel Integrated Approach of Energy Consumption Scheduling in Smart Grid Environment With The Penetration of Renewable Energy », *Int. J. Renew. ENERGY Res.*, vol. 5, n° 4, 2015.
- [2] S. Kahla, Y. Soufi, M. Sedraoui, et M. Bechouat, « Maximum Power Point Tracking of Wind Energy Conversion System Using Multi-objective Grey Wolf Optimization of Fuzzy-Sliding Mode Controller », *Int. J. Renew. ENERGY Res.*, vol. 7, n° 2, 2017.
- [3] D. Fendri et M. Chaabene, « Renewable energy management based on timed hybrid petri net approach for an isolated chalet application », *Int. J. Renew. Energy Res.*, vol. 6, n° 2, 2016.
- [4] M. N. Hassanzadeh et A. Safdarian, « Wind Energy Penetration with Load Shifting from the System Well - being Viewpoint », *Int. J. Renew. ENERGY Res.*, vol. 7, n° 2, 2017.
- [5] D. Astolfi, L. Scappaticci, et L. Terzi, « Fault diagnosis of wind turbine gearboxes through temperature and vibration data », *Int. J. Renew. Energy Res.*, vol. 7, n° 2, 2017.
- [6] C. G. Cooley et R. G. Parker, « The geometry and frequency content of planetary gear single-mode vibration », *Mech. Syst. Signal Process.*, vol. 40, n° 1, p. 91-104, 2013.
- [7] M. Zhao et J. Ji, « Dynamic analysis of wind turbine gearbox components », *Energies*, vol. 9, n° 2, p. 1-18, 2016.
- [8] J. Ooi, X. Wang, C. Tan, J. H. Ho, et Y. P. Lim, « Modal and stress analysis of gear train design in portal axle using finite element modeling and simulation », *J. Mech. Sci. Technol.*, vol. 26, n° 2, p. 575-589, 2012.
- [9] S. Draca, « Finite Element Model of a Double-Stage Helical Gear Reduction », Windsor, 2006.
- [10] W. Musial, S. Butterfield, et B. McNiff, « Improving Wind Turbine Gearbox Reliability », dans *European Wind Energy Conference*, 2007, p. 1-13.
- [11] F. Rasmussen, K. Thomsen, et T. Larsen, « The gearbox problem revisited », Roskilde, Denmark,



- 2004.
- [12] J. Lin et R. G. Parker, « Analytical characterization of the unique properties of planetary gear free vibration », *Vib. Acoust.*, vol. 121, n° 3, p. 316-321, 1999.
- [13] S. H. Gawande et S. N. Shaikh, « Experimental Investigations of Noise Control in Planetary Gear Set by Phasing », *J. Eng.*, vol. 2014, 2014.
- [14] T. M. Ericson et R. G. Parker, « Natural Frequency Clusters in Planetary Gear Vibration », *J. Vib. Acoust.*, vol. 135, n° 6, p. 061002-061002, 2013.
- [15] R. G. Parker, « Dynamic Response of a Planetary Gear System using a Finite Element / Contact Mechanics », *J. Mech. Des.*, vol. 122, p. 304-310.
- [16] S. S. Ghorpade, A. B. Kadam, D. A. Mane, S. H. Gawande, et S. N. Shaikh, « Dynamic Modeling of PGT using Analytical & Numerical Approach », *Mech. Des. Vib.*, vol. 3, n° 1, p. 24-30, 2015.
- [17] C. G. Cooley et R. G. Parker, « A Review of Planetary and Epicyclic Gear Dynamics and Vibrations Research », *Appl. Mech. Rev.*, vol. 66, n° 4, p. 40804, 2014.
- [18] A. Kahraman, « Natural modes of planetary gear trains », *Journal of Sound Vibration*, vol. 173. p. 125-130, 1994.
- [19] A. Kahraman, « Planetary Gear Train Dynamics », *J. Mech. Des.*, vol. 116, n° 3, p. 713, 1994.
- [20] J. Lin et R. G. Parker, « Sensitivity of Planetary Gear Natural Frequencies and Vibration Modes To Model », *J. Sound Vib.*, vol. 228, n° 1, p. 109-128, 1999.
- [21] A. Mohsine, E. M. Boudi, et A. El Marjani, « Modeling and Structural Analysis of Planetary Gear of a Wind Turbine », dans *3rd International Renewable And Sustainable Energy Conference (IRSEC)*, 2016, p. 1-5.
- [22] Errichello, R., 1979, "State-of-art review: gear dynamics", *Trans. ASME, J. Mech. Des.*, 101(3), 368- 372.
- [23] H. Nevzat Özgüven et D. R. Houser, « Mathematical models used in gear dynamics—A review », *Top. Catal.*, vol. 121, n° 3, p. 383-411, 1988.
- [24] P. K. Jena, « Static and Dynamic Analysis of Hcr Spur Gear Drive Using Finite Element Analysis », National Institute of Technology, 2009.
- [25] Z. Wei, « Stresses and Deformations in Involute Spur Gears By Finite Element Method », University of Saskatchewan Saskatoon, Saskatchewan, 2004.
- [26] G. hua Huang, S. si Xu, W. hua Zhang, et C. jin Yang, « Super-harmonic resonance of gear transmission system under stick-slip vibration in high-speed train », *J. Cent. South Univ.*, vol. 24, n° 3, p. 726-735, 2017.
- [27] Z. Zeng, J. Li, S. Zhang, Y. Hong, et Y. Wang, « Analysis of the Harmonic Response of a Modulation Permanent Magnetic Transmission Equipment Based on ANSYS », *Energy Power Eng.*, n° March, p. 63-70, 2015.